Contributors

Irasema Alcántara-Ayala
Instituto de Geografía, UNAM
Circuito Exterior, Ciudad Universitaria
04510, Coyoacán, México, D.F.
México

Gilles Arnaud-Fassetta
Université Paris-Diderot
Case Postale 7001
75205 Paris Cedex 13
France

Perry Bartelt
Avalanches, Debris Flows and Rockfall Research Unit
WSL Institute for Snow and Avalanche Research SLF
Flüelastrasse 11
CH-7260 Davos Dorf
Switzerland

Gerardo Benito
Laboratorio de Geomorfología e Hidrología
Centro de Ciencias Medioambientales, CSIC
Serrano 115 dup.
28006, Madrid
Spain

John Boardman
Environmental Change Institute,
SoGE, South Parks Road
Oxford, OX1 3QY
UK

Lisa Borgatti
Dipartimento di Ingegneria delle Strutture, dei Trasporti,
delle Acque, del Rilevamento, del Territorio
Alma Mater Studiorum Università di Bologna
Viale Risorgimento, 2
41036 Bologna
Italy

William B. Bull
6550 N. Camino Katrina
Tucson, AZ, 85718-2022
USA

Michael Bründl
Warning and Prevention Research Unit
WSL Institute for Snow and Avalanche Research SLF
Flüelastrasse 11
CH-7260 Davos Dorf
Switzerland

Etienne Cossart
UMR Prodig 8586 – CNRS
Université Panthéon-Sorbonne (Paris 1)
2 rue Valette,
75005 Paris
France

Michael Crozier
Victoria University of Wellington
School of Geography, Environment and Earth Sciences
PO Box 600
Wellington
New Zealand

Monique Fort
Université Paris Diderot (Paris7)
Département de Géographie
UFR GHSS, Case 7001
75205 Paris Cedex 13
France

Thomas Glade
Department of Geography and Regional Research
University of Vienna
Universitaetsstr. 7
A-1010 Vienna
Austria

Andrew S. Goudie
St Cross College
St Giles
Oxford, OX1 3LZ
UK

Avijit Gupta
School of Geography
University of Leeds
Leeds, LS2 9JT
UK

Francisco Gutiérrez
Universidad de Zaragoza
Departamento de Ciencias de la Tierra
Edificio Geológicas
C/. Pedro Cerbuna, 12
50009 Zaragoza
Spain

David Higgitt
National University of Singapore
Department of Geography
AS2, #03-01
1 Arts Link, Kent Ridge
117570 Singapore

Paul F. Hudson
Department of Geography and the Environment
University of Texas at Austin
Austin, TX 78712
USA

Gabi Hufschmidt
School of Geography
Victoria University of Wellington
P.O. Box 600
Wellington
New Zealand

Margreth Keiler
Department of Geography and Regional Research
University of Vienna
Universitaetsstr. 7
A-1010 Vienna
Austria

Molly McGraw
Southeastern Louisiana University
SLU-10686
Hammond, LA 70402
USA

David Petley
Durham University
Department of Geography Science Laboratories
South Road
Durham, DH1 3LE
UK

Jürg Schweizer
Warning and Prevention Research Unit
WSL Institute for Snow and Avalanche Research SLF
Flüelastrasse 11
CH-7260 Davos Dorf
Switzerland

Olav Slaymaker
University of British Columbia
Department of Geography
1984 West Mall
Vancouver, V6T 1Z2
Canada

Mauro Soldati
Dipartimento di Scienze della Terra
Università di Modena e Reggio Emilia
Largo S. Eufemia, 19
41000 Modena
Italy

Jean-Claude Thouret
Laboratoire Magmas et Volcans UMR 6524 CNRS et OPGC
Université Blaise Pascal Clermont II
5 rue Kessler
63038 Clermont-Ferrand cedex
France

Cees J. van Westen
International Institute for Geo-Information Science and Earth Observation (ITC)
Hengelosestraat 99
PO Box 6
7500 AA Enschede
The Netherlands

Heather Viles
School of Geography and the Environment
South Parks Road
Oxford, OX1 3QY
UK

Harley J. Walker
Department of Geography and Anthropology
Louisiana State University
Baton Rouge, LA 70803
USA

Yang Xiaoping
Institute of Geology and Geophysics
Chinese Academy of Sciences
P.O. Box 9825
Beijing 100029
China

7 Catastrophic landslides and sedimentary budgets

Monique Fort, Etienne Cossart, and Gilles Arnaud-Fassetta

Landslides are a dominant geomorphic process affecting mountain slopes worldwide (see also Chapters 6 and 8). They represent a major sediment source that can supply a large amount of unstable debris to river channels and may affect the fluvial sediment yield. A distinctive part of the geomorphic evolution of active mountain belts, catastrophic landslides generally develop very rapidly so that they are among the most powerful natural hazards on Earth. By temporarily or persistently impounding river channels, they delay or block the delivery of sediments, affect the (dis)continuity of the cachment-scale sediment cascade, and exert a control over the fluvial valley systems (Hewitt, 2002; Korup *et al*., 2004). As a consequence, landslides may generate indirect hazards along fluvial systems, so that they represent a major threat to settlements, infrastructures and catchment management that may be felt over long distances from the unstable area (Plafker and Eriksen, 1978; Li *et al*., 1986; Costa, 1991; Korup, 2005; Hewitt *et al*., 2008). Their magnitudes, together with their causative factors, suggest the difficulty, if not the impossibility, of preventing and/or to predicting them.

In this brief overview, we shall firstly define catastrophic landslides and their geomorphic impacts, with special attention given to landslide-induced dams; we shall move on to their influence on sediment budgets, at local and basin-wide scales, before eventually considering a few actions that may help to minimize the vulnerability and risks for the potentially affected populations.

7.1 Catastrophic landslides: definition, modes of emplacement and geomorphic significance

7.1.1 Definition

The term landslide covers a large array of features. Catastrophic landslides (also referred to as super-large or giant landslides in the literature) are considered here as low frequency, massive rock slope failures characterized by their magnitude, the rapidity of their emplacement and by their spatial and temporal impacts on geomorphic systems. More specifically, the magnitude of catastrophic landslides refers either to the depth of the sliding place, to the scar area or the total disturbed area, including the deposition zone, or to their volume (Table 7.1). The displaced material generally covers at least five orders of magnitude between 10^5 and 10^{10} m^3 (Evans *et al*., 2006; Hewitt *et al*., 2008).

Determination of landslide volumes can be assessed directly from field data. Alternatively, at a basin-wide scale, digital elevation models (DEMs) are useful tools but they require good positional accuracy (Korup, 2005). Aerial photo measurements (based mostly on the total affected area) allow the production of an exhaustive inventory, and time series analysis, yet their use necessitates photogrammetric modelling and ground truthing; also, the fast recovery by the vegetation in some (tropical) mountains may lead to an underestimate of the final area/volume (Brardinoni and Church, 2004; Koi *et al*., 2008) and introduce biases in magnitude/frequency estimation. Despite this limitation, a number of analyses of landslide magnitude/frequency relations have shown they are scale invariant and they obey a power law of the general form $N(A) \approx A^{-b}$, where A is landslide area, $N(A)$ the number of events of greater than a given volume, and b is a constant (Hovius *et al*., 2007). This equation is used to quantify the distribution of landslides in space and time, and hence their density and recurrence.

7.1.2 Occurrence and modes of emplacement of catastrophic landslides

Landslide occurrence depends on various controls: climate, slope steepness, relief amplitude, bedrock geology, failure plane orientation, vegetation and landuse cover, etc.

Geomorphological Hazards and Disaster Prevention, eds. Irasema Alcántara-Ayala and Andrew S. Goudie. Published by Cambridge University Press. © Cambridge University Press 2010.

TABLE 7.1 *Selected catastrophic landslides of the twentieth century and their impacts*

Year	Location	Landslide volume (m^3)	Trigger	Impacts	Comments
1911	Usoi rockslide (Tadjikistan)	2.2×10^9	M 7.4 Pamir earthquake	54 killed; Lake Sarez, the largest natural landslide dam in the world (>60 km long, >500 m depth, volume 17×10^9 m^3) across the Murgab River	Concerns about a possible failure of the dam, that would affect >5 million people along the Bartang–Pyanj–Amu Daria watershed
1933	Diexi, Sichuan province (China)	150×10^6	M 7.5 earthquake	>2,400 killed; dam of the Min River for 45 days (lake volume: $400 \times 10^6 m^3$)	Draining of the lake by overspilling; the flood propagated >250 km downstream (average velocity 5.5–7 m/s)
1959	Malpasset, Fréjus (France)	30×10^6	Heavy precipitation	423 killed; railway damaged along 2.5 km; 50 farms destroyed	Inadequate artificial dam, built against weaken bedrock (foliated and tectonized schists + non-identified faults)
1963	Vaiont rockslide (Italy)	270×10^6	Precipitation + high water level followed by rapid lake drawdown	2000 killed; rockslide failed in the 150×10^6 m^3 Vaiont reservoir, resulting in a catastrophic flood (city of Langarone badly damaged, together with 4 other villages)	A 100 m high wave of water overtopped the doubly curved arch of hydroelectric power dam; possible reactivation of a relict landslide; brittle failure of clays in depth
1967	Tanggudong debris slide, Sichuan (China)	68×10^6		Dam of the Yalong River; lake volume 600×10^6 m^3	Catastrophic failure of the dam
1970	Nevado Huascaran rock debris/avalanche (Peru)	$30–50 \times 10^6$	M 7.7 earthquake	>18,000 killed; city of Yungay destroyed	Average velocity 280 km/hr; same peak already affected by the same type of failure in 1962 (4,000–5,000 killed)
1980	Mount St Helens debris avalanche (USA)	2.8×10^9	Volcanic eruption	5–10 killed, most people evacuated; destruction of infrastructure; Spirit Lake (258×10^9 m^3) dammed	Rotational rock slide, followed by 23 km long debris avalanche; average velocity 125 km/hr; dam artificially stabilized by an outlet tunnel
1983	Thistle debris slide (USA)	21×10^6	Snowmelt and heavy rain	Destruction of infrastructure; dam of the Spanish Fork River; lake volume 78×10^6 m^3	Heavy economic losses ($US 600 million); lake permanently drained by human intervention
1983	Sale Mountain landslide, Gansu Province (China)	30×10^6	No obvious trigger	237 killed, 3 villages destroyed; toe of the displaced mass across the 800 m wide valley of the Baxie river	Mudstone and loess material; composite landslide, with progressive failure and increasing velocity up to 20 m/s
1984	Mount Ontake (Japan)	36×10^6	M 6.8 earthquake	Travel distance of 13 km down to adjacent valleys	Failure of the southeastern flank of Mt Ontake volcano, transformed into a lahar (estimated volume 56×10^6 m^3); velocity 22–36 m/s

1985	Bairaman debris avalanche (Papua New Guinea)	180×10^6	M 7.1 earthquake	210 m high landslide dam; lake (volume 50×10^6 m^3) artificially drained; villagers evacuated	Debris flow volume 120×10^6 m^3; average velocity 20 km/hr; affected 39 km Bairaman River down to Salomon Sea
1985	Catastrophic lahar, Nevado del Ruiz (Columbia)	90×10^6	Snowmelt lahar triggered by volcanic eruption	>23,000 killed (buried city of Armero, 40 km distant); small eruption ($<5 \times 10^6$ m^3 magma ejected), but large amount of meltwater (38–44×10^6 m^3) released in 20–90 min	Lahar velocity in the Lagunillas valley, 50 to 80 km/hr; peak flow velocities 5–15 m/s; lahar reached 104 km in 4 hours; economic losses ($US 1 billion); former destructive lahar in 1845, with same areas affected
1987	Val Pola landslide (Italy)	40×10^6	Cumulative and unusually severe rainfall	27 killed and destruction of many buildings ($US 400 million); damming of the Adda River valley	The rock-valanche produced a wave of muddy water 2.7 km upstream; velocity 248–310 km/h; spillway tunnel constructed
1991	Randa rockfall (Switzerland)	20×10^6	Melting of permafrost?	Dam of the Vispa River, flooding of the Randa village	Continuous rockfall lasting several hours, with exponential acceleration before final movement
1993	La Josephina landslide (Ecuador)	$20–44 \times 10^6$	Rainfall	Dam of the Paute River; lake volume 177×10^6 m^3; drained out catastrophically; 71 killed, most people evacuated before lake breakout	Flood propagated >60 km downstream; peak discharge: 9,000–14,000 m^3/s; 13×10^9 m^3 solid load; velocity 5–20 m/s; heavy economic losses ($US 147 millions)
1999	Malpa rockfall and debris flow (India)	1×10^6	High intensity rainfall	221 killed; Malpa River dammed, followed by an outburst flood	Former landslides at the same site; proximity of the Main Himalayan Thrust Fault
1999	Mt Adams, South Westland (New Zealand)	$10–15 \times 10^6$	No obvious trigger	Dam formed in the lower Poerua River gorges; massive fanhead aggradation at the mountain range front	Outburst flood within less than one week (peak discharge 1,000–3,000 m^3/s); persistent postfailure aggradation
2000	Yigong debris slide and debris flow, Tibet Province (China)	300×10^6	Excessive rainfall and snow-melt waters	Landslide dam of the Yigong River; natural breach caused catastrophic flood (peak discharge 120,000 m^3/s); loss of property and infrastructure downstream to India	Failure very similar to the 1900 Yigong, large (5.1×10^8) landslide and resulting dam and lake
2007	Guinsaugon rockslide–debris avalanche, Leyte Island, Philippines	15×10^9	No specific trigger but heavy rainfall in the preceding days	Disintegration of slidden mass; average thickness of debris 10 m; runout distance 3,800 m; >1,000 casualties when Guinsaugon village, located on flat valley floor, was buried under 4–7 m deep debris.	Failure of 450 m high, forested rock slope located within active Philippine fault zone (sheared and brecciated rocks); runout distance enhanced by friction reduction when debris ran over flooded paddy fields; estimated and simulated mean velocity 27–38 m/s and 35m/s respectively.

(Cruden and Varnes, 1996; Dikau *et al*., 1996). The world-wide distribution of catastrophic landslides shows a good correlation with mean local relief greater than 1000 m (which makes up over 5% of Earth's land surface; Korup *et al*., 2007), with seismo-tectonically active mountains (e.g. Central and High Asia, New Zealand Alps, Coastal Ranges) or volcanic belts (Pacific Rim), and with recently deglaciated mountain slopes (Evans and Clague, 1994).

A large number of catastrophic rock failures consist of rock avalanches (or sturzstroms; Hsü 1975) and/or rock-slides, even if other processes such as translational rock-slides, rotational slumps or spreads cannot be excluded. The mode of emplacement of rock avalanches can be very complex: it generally involves an initial failure from steep mountain walls of cohesive rock mass that descends several hundreds or thousands of metres and is disintegrated and crushed, a process that gives great momentum to the resulting debris (Hewitt, 2002). The nature and extent of the resulting deposits depend on the geological setting and valley morphology (Costa and Schuster, 1988). In topographically confined settings, the deposits may pile up on and run up the opposing slope, or split into separate lobes both upstream and downstream of the impacted slope, all situations that favour the blockage of the valley and the formation of a lake. Alternatively, wherever there is no spatial confinement, the crushed rocks may travel long distances and evolve, in the presence of water (or snow, or ice), into giant debris flows (Plafker and Eriksen, 1978; Fort, 1987; Shang *et al*., 2003). These failures may also incorporate a variety of earth materials entrained in their path, and the runout process may affect, or be affected by, the type of substrate (Hewitt, 2002; Schneider *et al*., 2004).

Earthquakes and/or high intensity precipitation are the most efficient triggering factors for rapid collapse. The failure site may be controlled by major tectonic lines (Figure 7.1; Fort, 2000), or be considered as a direct adjustment to high rates of rock uplift and correlated river incision (Burbank *et al*., 1996). The failure may be preceded by a phase during which slow, deep-seated deformation leads to the opening of tension cracks, weakening of the shear strength of the rock mass, and eventually to high pore-water pressures. Other unusual mechanisms such as acoustic fluidization during sliding, or internal, self-accelerating rock fracture (Kilburn and Petley, 2003) may also favour large-scale rock slope failures (Hewitt *et al*., 2008). Additionally, anthropogenic actions may be the cause of large hillslope destabilization (e.g. Vaiont reservoir; Table 7.1).

These very large rock mass failures are generally considered as a major denudational process of active orogens, and as formative events influencing landscape development (Brunsden and Jones, 1984; Fort, 1988, 2000; Hewitt, 1988, 1998, 2002; Fort and Peulvast, 1995; Burbank *et al*., 1996; Korup *et al*., 2004, 2007). More specifically, they give rise to complex sedimentary assemblages and to specific constructional and erosional landforms that create 'interrupted valley landsystems' distinctive of these large-scale landslides (Hewitt, 2006).

7.2 Geomorphic impacts of catastrophic landslides

Catastrophic landslides have direct geomorphic impacts at the local, basin-wide and mountain-belt scales, as synthesized by Costa and Schuster (1988), Hewitt (2002, 2006) and Korup (2005). We want to stress here local and regional impacts, which are the most meaningful in terms of hazards and risks for the population. Geomorphic impacts and their consequences on water and sediment fluxes and budgets will be appreciated in considering different interactions between landslides and fluvial systems.

7.2.1 Interactions with river systems

Three different situations are illustrated: partial blockage of the valley by the landslide, complete damming and upstream water ponding, and catastrophic collapse of the landslide dam (Figure 7.2).

In the case of partial blockage (Figure 7.2, case 1), the landslide mass forces the river to divert its course to the opposite bank; this in turn leads to a change in transverse and longitudinal channel geometry, channel pattern and morphology. Wherever the opposite bank consists of soft material (slope or alluvial deposits), this diversion triggers bank erosion and further destabilizes the entire hillslope (Figure 7.2B). Upstream of the landslide mass, which acts as the local base level, braiding of the river and aggradation predominate. These may indirectly increase overflow and channel avulsion-shifting frequencies, and flood hazards for the adjacent settlements (Figure 7.2A). Across the landslide mass, the narrower cross section of the river favours erosion of the landslide debris and increases sediment fluxes downstream, whereas the larger blocks exceeding the competence of the stream power form a debris lag, which armours the channel bed and prevents further erosion during regular high flows.

When the volume of the landslide is sufficient to block the valley entirely (Figure 7.2, case 2 and Figure 7.2D), a lake will instantaneously start filling up, whereas the downstream part is starved of water. Lake depth depends on valley geometry and landslide height; the latter may reach hundreds of metres (e.g. Lake Sarez; Table 7.1). Landslide dams may be ephemeral (a few minutes to a few hours), or

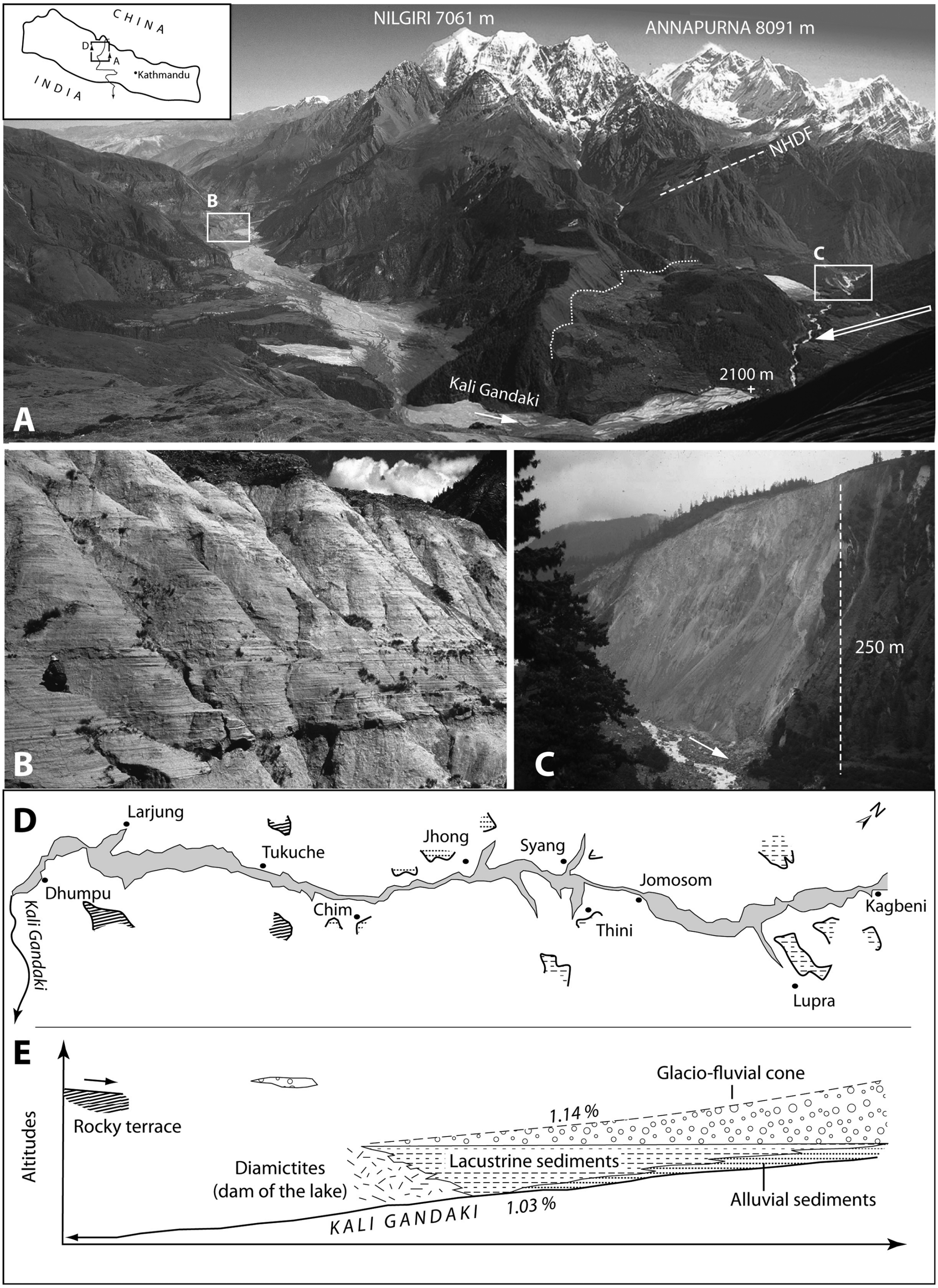

FIGURE 7.1. The large, prehistoric Dhumpu–Kalopani rock avalanche and its morpho-sedimentary impacts (Nepal Himalayas). The collapsed mass failed along the North Himalayan Detachment Fault (NHDF) and blocked durably the Kali Gandaki River, which had carved the deepest gorges in the world across the Annapurna (8091 m) and Dhaulagiri (8172 m) ranges. The 23 km long, >200 m deep Marpha lake developed and filled in with sediments brought from upstream and from glaciated tributary valleys. The braided pattern of the river course reflects the still persisting role of the rock-avalanche barrier in the denudational evolution of the mountain.

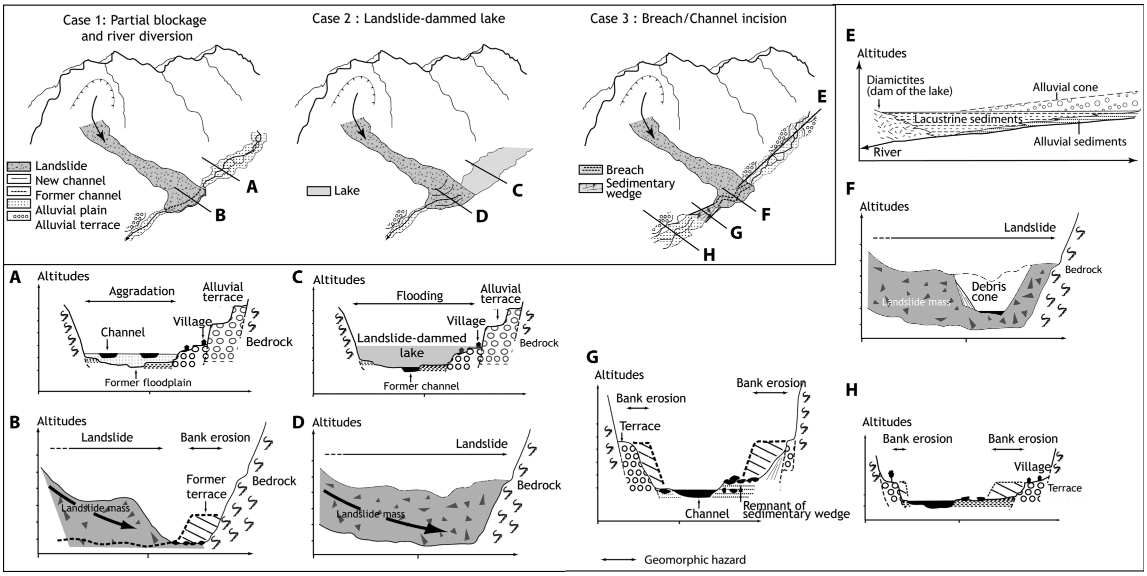

FIGURE 7.2. Types of geomorphic impacts of landslide dams on hydrosystems.

short-term (a few weeks or months), or persistent (several thousand years), a duration that directly influences their potentially catastrophic nature and their control on sediment fluxes and budgets (Figure 7.1 and Figure 7.2E). Dam longevity is a function of its stability, which depends on the size and shape of the dam, the characteristics of the geological material composing the dam (material properties, grain size distribution), the volume and rate of water and sediment inflow to the newly formed lake, and the rate of seepage through the dam (Costa and Schuster, 1988). Water ponding occurs up to the dam height, resulting in upstream backwater flooding that can be damaging for settlements and infrastructures (Figure 7.2C). The rapidity of the water level rise depends on the river inflow versus the size and shape of the inundated valley; it generally leaves enough time for evacuation of the threatened populations to take place.

In contrast, catastrophic downstream flooding (Figure 7.2, case 3) will occur following a rapid failure of the landslide dam, caused either by overtopping and immediate retrogressive incision across the dam (Figure 7.2F), or by increasing shear stress because of seepage at the base of the dam (that can be reinforced by the weight of the impounded water mass upstream), or by displacement waves triggered by landslide failures directly into the lake. The catastrophic nature of the (flash)flood, involving the release of a large amount of sediments and water, is recorded by extreme peak discharges (usually back-calculated from field surveys and hydraulic equations) and high velocities that permit the transport of sediments derived from the dam and from the upstream lacustrine reservoir. The geometry and extent of the coarse debris wedge formed immediately downstream of the dam (Figure 7.2G) suggest both the competence of the debris laden waters (often in the form of debris flows) and their rapid evolution in both time and space into hyper-saturated flows and then into 'normal' high flows, in relation to progressive deposition of the coarser material in the flood plain (Figure 7.2H).

The catastrophic draining of a landslide-dammed lake and associated flooding may create secondary impacts. Firstly, new landslides may develop, both upstream of the lake, following the rapid drawdown of the water, and across and downstream of the dam, where the propagation of the flood contributes over very large distances to a sudden rise of water, bank undercutting and hillslope instabilities (e.g. Yigong debris flow; Table 7.1), which may in turn give rise to new dams and flooded areas. Secondly, specific aggradational landforms may develop, such as 'barrier-defended' terraces upstream of the dam, with the sedimentary facies reflecting the architecture and sequences of debris inputs from the trunk river and adjacent tributaries and slopes (Hewitt, 2002). Thirdly, a distinctive morphology of 'interrupted valleys' appears as a legacy of past catastrophic events, consisting of partial obstructions by landslide barriers (e.g. boulder accumulations resting in the middle of river channels) or in persistent impoundments that 'create a chronically fragmented drainage system' (Hewitt, 2006). This is the case for the Dhampu–Chooya–Kalapani rock avalanche that dammed the upper Kali

Gandaki valley (Nepal Himalaya) some 70,000 years ago and is still influencing the bed profile and planform pattern (braiding) of the river channel (Fort, 2000) (Figure 7.1). This influence is related not only to the stability of the dam, but also depends on the stream power of the river being sufficient to breach the dam. This is a function of the longitudinal profile, and of the liquid and solid discharge of the river (parameters controlled by climate, autocyclic processes, slope and tectonics).

7.2.2 Impacts on sedimentary fluxes and budgets

In the frame of sedimentary budgets, landslide masses form a particular type of sediment store, characterized by their volume and calibre of materials, and by their distance from the channel (Slaymaker, 2006). As already mentioned, large landslides impact adjacent channels and valleys, either by accelerating, or slowing down, or even interrupting, the conveyance of sediment to the downstream reservoirs. These different impacts may occur successively in time, depending on the magnitude of the landslides and their capacity to act or not as an efficient barrier; they may randomly affect the functioning of the sediment fluxes, and contribute to the formation of a cascading sequence of intramontane storage units (Korup, 2005).

Local scale

An illustration is provided by the sedimentary budget of the upper Cerveyrette catchment (Southern French Alps). This was directly influenced by a series of earth-flows that developed after glacial retreat, and was caused by the combined effects of post-glacial debuttressing and liquefaction of the serpentinite bedrock, in a context of seismic activity (Cossart and Fort, 2008) (Figure 7.3A). The largest slide-earth flow of the Chenaillet (*c*. $3 \times 10^7\,m^3$; 3.5 km long) efficiently dammed the valley, so that the Bourget Plain developed in response to the impoundment. Longitudinally, the trap was infilled with alluvial gravels and silts fed by alpine periglacial and/or still-glaciated hillslopes. This debris accumulated as a prograding fan delta encroaching upon the lake that developed in the distal part of the valley, closest to the dam. Lacustrine deposits are interfingered with colluvial debris derived from the steep slopes of Mount Lasseron as scree and avalanche cones.

The sediment budget was estimated by combined field surveys, DEM and GIS approaches (Figure 7.3B; Cossart and Fort, 2008). The sediment stored in the Bourget Plain represents approximately the same volume ($22.3 \times 10^6\,m^3$) as the Chenaillet landslide dam ($21 \times 10^6\,m^3$), whereas debris still blankets the hillslopes ($18.4 \times 10^6\,m^3$) without reaching the Bourget Plain. This store developed between the Late Pleistocene and *c*. 5,000 BP; it first interrupted, then considerably reduced the sediment fluxes downstream. As soon as the blockage of the valley occurred, the downstream part of the Cerveyrette torrential river started adjusting its longitudinal profile by retrogressive erosion. The present situation corresponds to a total sediment removal and export of only $10^6\,m^3$ (*c*. 1/60 of the debris). However, sporadic dissection of the landslide dam triggered by extreme meteorological events is directly threatening the Cervières village, as during the 1957 >100-years recurrence flood that destabilized the entire hydrosystem. This example shows how, in alpine headwater contexts, landslide dams are persistent features controlling the sediment fluxes long after their occurrence.

Regional scale

Large landslides may contribute to a significant increase in sediment yield in a very short period following failure, not only by direct massive input of landslide debris into the fluvial system, but also by secondary hillslope processes that rework the landslide material before vegetation regrowth. Such landslide-derived sediment pulses result in aggradation in the downstream reaches from the landslide site, and are often accompanied by metamorphosis and/or change in the river course that may induce off-site hazards and damaging impacts to downstream settlements and infrastructures. For instance, Korup *et al*. (2004) calculated that the 1999 Mount Adams rock avalanche (New Zealand) produced a specific sediment yield in excess of approximately $75{,}700 \pm 4{,}600\ t\ km^{-2}\ a^{-1}$, as expressed by the massive fanhead aggradation and the opening of a major avulsion channel at the mountain range front. This sediment yield represents a sediment discharge of $2.5 \times 10^6\ m^3\ a^{-1}$ calculated for the three years following failure, an amount that rapidly declined after the event. In the Nepal Himalayas, Fort (1987) described a giant ($>4 \times 10^9\ m^3$) collapse of the south face of the Annapurna IV peak that occurred about 500 years ago, and filled the 35 km distant Pokhara valley under a 60 to 100 m thick gravel aggradation, which blocked and caused the flooding of adjacent tributary valleys. The calculated annual contribution of Annapurna rockslide-derived sediment is in the order of $4 \times 10^6\,m^3\,a^{-1}$ and represents, for the upper catchment, a sediment yield of $22{,}860\,m^3\ a^{-1}\ km^{-2}$ (Fort, 1987; Fort and Peulvast, 1995). This is a figure averaged over a 500-year period, which in fact is exceptionally high if one considers the fact that the aggradation took place in a very short time, i.e. 'instantaneously' after the failure.

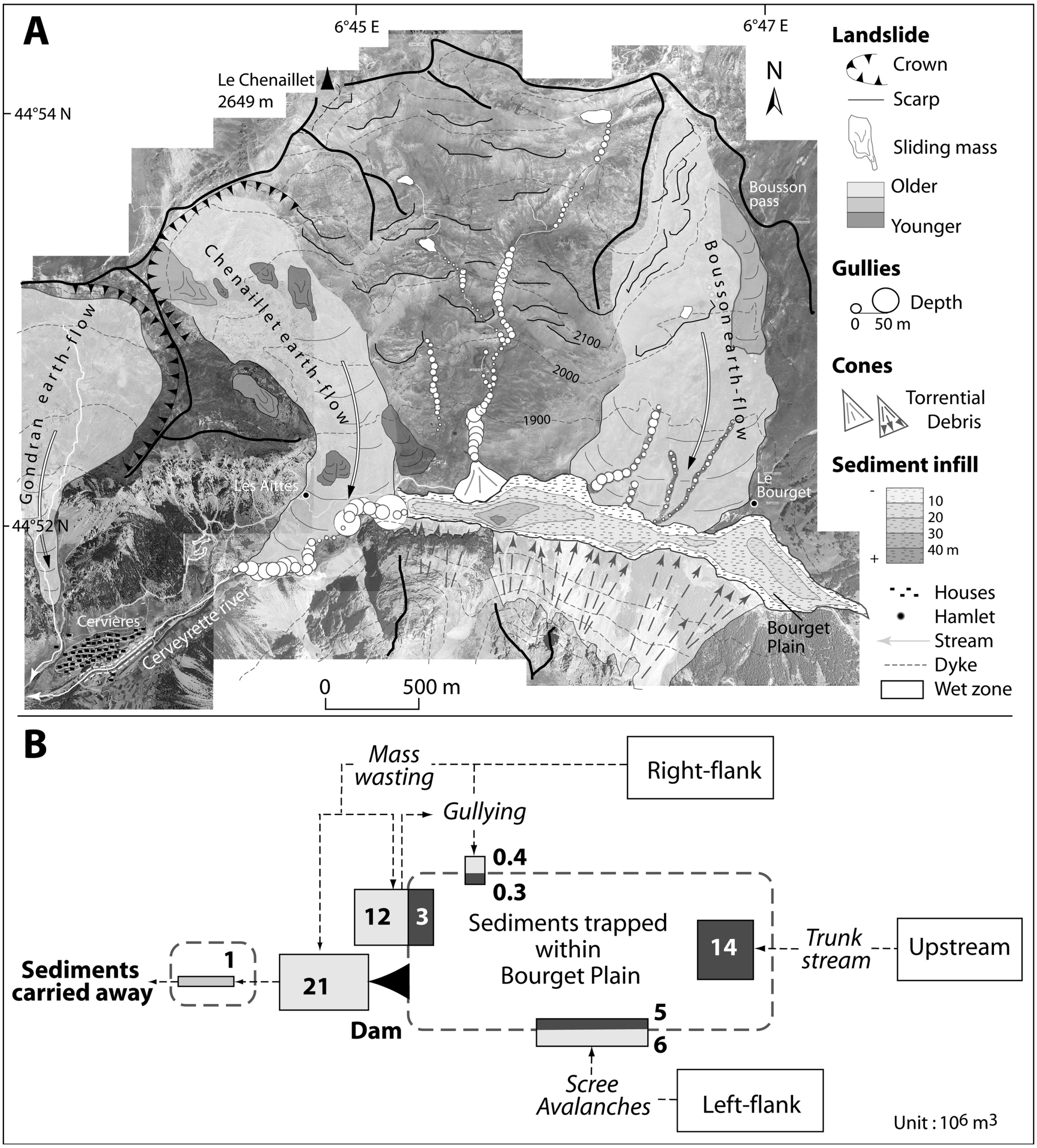

FIGURE 7.3. Sedimentary budget assessment in response to the Chenaillet earthflow dam (French Southern Alps). (Modified and completed after Cossart and Fort (2008.)

7.3 Forecasting and preventing

Catastrophic rock failures are generally preceded by periods of accelerated creep, which may result in observable slope deformation and 'sackung' related features: development and widening of tension cracks, buckling, increased rockfall activity and toppling, or break-out across bedding. Measured stress drops in crustal rock, and related fracturing could provide a physical basis for quantitatively forecasting catastrophic slope failure (Kilburn and Petley, 2003). However, monitoring of all potential threatening slopes is not realistic, especially in developing countries where other priorities (food, shelter, employment) come well ahead of unpredictable natural hazards.

Other forecasting methods are based on statistical assessment of landslide susceptibility; they rely on a series of variables (landslide inventory with the help of GIS, terrain predisposing factors, neo-predictive variables with a geomorphological meaning) that are tested (simulations) and eventually evaluated by expert judgement (Thiery *et al.*, 2007). Another similar approach is based on geotechnical modelling and 3-D model calibration set up from a known and well-studied event (quantitative data), as was done after the 1987 Val Pola landslide, one of the most destructive and costly natural disasters that has occurred in Italy during recent decades (Costa, 1991; Crosta *et al.*, 2004). In their study, Crosta *et al.* (2004) showed how modelling techniques help one to understand the rheology of such a failure, and to predict its timing in highlighting the transformation of potential energy to kinematic energy.

The power law curve of landslide magnitude/frequency can also be used for landslide hazard assessment (Evans *et al.*, 2006), and as input into a quantitative risk calculation if combined with vulnerability data, as was done to assess rockfall risk along transportation corridors (Hungr *et al.*, 1999).

To prevent the failure of landslide dams and resulting catastrophic floods, the most commonly used control measure consists of the construction of spillways either across the landslide crest or across the adjacent bedrock. Alternatively, drainage by siphon pipes, pump systems or diversion tunnels (Val Pola, Mount St Helens, Bairaman; Table 7.1) are short-term measures to control lake level. More radical methods consist in large-scale blasting, as was done across the landslide dams that were formed near Beichuan city after the 18 May 2008 Sichuan earthquake in China. However, the disaster may occur before adequate control measures can be completed (more particularly in remote and rugged areas that render transport of heavy equipment very difficult), or because high rapid inflow to the impoundment often exceeds general predictions and causes an early dam failure (Shang *et al.*, 2003). In the case of Lake Sarez and the related Usoi landslide dam (Tadjikistan), the highest dam on Earth, and despite extensive observations and technical studies that suggest a satisfactory stability of the dam against sliding, the possibility of a catastrophic outburst flood that would destroy the many villages and infrastructures of the Bartang–Pyang–Amu Darya catchment, situated between the lake and the Aral Sea, cannot be entirely ruled out (>5 million people would be affected). Combined measures are thus being implemented, consisting of (i) the monitoring of the stability of the dam and slopes surrounding the lake, (ii) an early warning system to alert inhabitants of the upper Amu Darya valley, together with (iii) the modelling of a series of flood scenarios to determine the degree of risk and vulnerability of downstream villages and infrastructures (Alford and Schuster, 2000). Whatever these measures, a simple doubling of the present mean streamflow volume of 2000 $m^3 s^{-1}$ of the Bartang River would readily destroy large portions of existing roads, low-lying villages and agricultural land for more than 100 km downstream from the dam, whereas a lake outburst flood would generate an instantaneous, catastrophic peak flow of about one million cubic metres per second (Alford and Schuster, 2000).

7.4 Conclusions

Despite their low frequency, large landslides are natural hazards that induce geomorphic impacts that can badly damage human settlements (Table 7.1). They are generally associated with episodes of extreme rainfall and/or with earthquakes, which are the natural hazards that cause the highest human losses on Earth. The rapid failure of a landslide dam will cause catastrophic downstream flooding whereas a long-lasting dam and its resulting filling by sediments will mostly affect mountain valley morphology and the sediment cascade.

The development of large-scale, catastrophic landslides should be put in the broader, long-term perspective of the evolution of a mountain range. In the context of the overall balance between erosion and rock uplift rates (Burbank *et al.*, 1996; Montgomery, 2001), superficial variables such as sediment fluxes and hillslope angle respond to both climate forcing and sporadic, catastrophic mountain slope collapse. This results in punctuated epicycles of aggradation and/or river incision that offset the equilibrium state at a shorter, 10^4–10^5 year time-scale (Fort, 1988; Pratt-Sitaula *et al.*, 2004). These high magnitude, low frequency failures are the very ‘formative events’ of the present morphology of active mountains and accomplish the main part of the denudation process of these orogens.

References

Alford, D. and Schuster, R. L. (2000). Introduction and summary. In *Usoi Landslide Dam and Lake Sarez: An Assessment of Hazard and Risk in the Pamir Mountains, Tajikistan*. United Nations, ISDR Prevention Series n°1, 1–18.

Brardinoni, F. and Church, M. (2004). Representing the landslide magnitude-frequency relation: Capilano river basin, British Columbia. *Earth Surface Processes and Landforms*, **29**, 115–124.

Brunsden, D. and Jones, D. K. C. (1984). The geomorphology of high magnitude-low frequency events in the Karakoram mountains. In K. J. Miller (ed.), *The International Karakoram Project*, vol. 1, Cambridge: Cambridge University Press, pp.383–388.

Burbank, D. W., Leland, J., Fielding, E. *et al*. (1996). Bedrock incision, rock uplift and threshold hill slopes in the northwestern Himalayas. *Nature*, **379**, 505–510.

Cossart, E. and Fort, M. (2008). Consequences of landslide dams on alpine river valleys: examples and typology from the French Southern Alps. *Norsk Geografisk Tidsskrift (Norwegian Journal of Geography)*, **62**, 75–88.

Costa, J. E. (1991). Nature, mechanics, and mitigation of the Val Pola landslide, Valtellina, Italy 1987–1988. *Zeitschrift für Geomorphologie*, **35**, 15–38.

Costa, J. E. and Schuster, R. L. (1988). The formation and failure of natural dams. *Geological Society of America Bulletin*, **100**, 1054–1068.

Crosta, G. B., Chen, H. and Lee, C. F. (2004). Replay of the 1987 Val Pola Landslide, Italian Alps. *Geomorphology*, **60**, 127–146.

Cruden, D. M. and Varnes, D. J. (1996). Landslide types and processes. In *Landslides, Investigation and Mitigation*. Washington, DC: National Academy Press, 36–75.

Dikau, R., Brunsden, D., Schrott, L. and Ibsen, M. (eds.) (1996). *Landslide Recognition: Identification, Movement and Causes*. New York; Chichester: Wiley.

Evans, S. G. and Clague, J. J. (1994). Recent climatic change and catastrophic geomorphic processes in mountain environments. *Geomorphology*, **10**, 107–128.

Evans, S. G., Scarascia Mugnozza, G., Strom, A. L. *et al*. (2006). Landslides from massive rock slope failure and associated phenomena. In S. G. Evans *et al*. (eds.), *Landslides From Massive Rock Slope Failure*, Dordrecht: Springer, pp. 3–52.

Fort, M. (1987). Sporadic morphogenesis in a continental subduction setting: an example from the Annapurna Range, Nepal Himalaya. *Zeitschrift für Geomorphologie Supplement-Band*, **63**, 9–36.

Fort, M. (1988). Catastrophic sedimentation and morphogenesis along the High Himalayan front: implications for palaeoenvironmental reconstruction. In P. Whyte, J. S. Aigner, N. G. Jablonski *et al*. (eds.), *The Palaeoenvironment of East Asia from Mid-Tertiary*, Centre of Asian Studies, University of Hong Kong, pp.170–194.

Fort, M. (2000). Glaciers and mass wasting processes: their influence on the shaping of the Kali Gandaki valley (higher Himalaya of Nepal). *Quaternary International*, **65**/66, 101–119.

Fort, M. and Peulvast, J.-P. (1995). Catastrophic mass-movements and morphogenesis in the Peri-Tibetan Ranges: examples from West Kunlun, East Pamir and Ladakh. In O. Slaymaker (ed.), *Steepland Geomorphology*. Chichester: Wiley, 171–198.

Hewitt, K. (1988). Catastrophic landslide deposits in the Karakoram Himalaya. *Science*, **242**, 64–67.

Hewitt, K. (1998). Catastrophic landslides and their effects on the Upper Indus streams, Karakoram Himalaya, northern Pakistan. *Geomorphology*, **26**, 47–80.

Hewitt, K. (2002). Postglacial landforms and sediment associations in a landslide-fragmented river system: the Transhimalayan Indus stream, Central Asia. In K. Hewitt, M. L. Byrne, M. English and G. Young (eds.), *Landscapes of Transition: Landform Assemblages and Transformations in Cold Regions*. Dordrecht: Kluwer, pp. 63–91.

Hewitt, K. (2006). Disturbance regime landscapes: mountain drainage systems interrupted by large rockslides. *Progress in Physical Geography*, **30**, 365–393.

Hewitt, K., Clague, J. J. and Orwin, J. F. (2008). Legacies of catastrophic rock slope failures in mountain landscapes. *Earth Science Reviews*, **87**, 1–38.

Hovius, N., Stark, C. P. and Allen, P. A. (2007). Sediment fluxes from a mountain belt derived by landslide mapping. *Geology*, **25**, 231–234.

Hsü, K. J. (1975). Catastrophic debris streams (sturzstroms) generated by rockfalls. *Geological Society of America Bulletin*, **86**, 129–140.

Hungr, O., Evans, S. G. and Hazzard, J. (1999). Magnitude and frequency of rockfalls and rock slides along the main transportation corridors of Southern British Columbia. *Canadian Geotechnical Journal*, **36**, 224–238.

Kilburn, C. R. J. and Petley, D. N. (2003). Forecasting giant, catastrophic slope collapse: lessons from Vajont, Northern Italy. *Geomorphology*, **54**, 21–32.

Koi, T., Hotta, N., Ishigaki, I. *et al*. (2008). Prolonged impact of earthquake-induced landslides on sediment yield in a mountain watershed: the Tanzawa region, Japan. *Geomorphology*, **101**, 692–702.

Korup, O. (2005). Geomorphic imprint of landslides on alpine river systems, southwest New Zealand. *Earth Surface Processes and Landforms*, **30**, 783–800.

Korup, O., McSaveney, M. and Davies, T. R. H. (2004). Sediment generation and delivery from large historic landslides in the Southern Alps New Zealand. *Geomorphology*, **61**, 189–207.

Korup, O., Clague, J. J., Hermanns, R. L., *et al*. (2007). Giant landslides, topography, and erosion. *Earth and Planetary Science Letters*, **261**, 578–589.

Li, T., Schuster, R. L. and Wu, J. (1986). Landslide dams in south-central China. In R. L. Schuster (ed.), *Landslides Dams: Processes, Risk, and Mitigation*. American Society of Civil Engineers, Geological Special Publication, 3, pp. 21–41.

Montgomery, D. R. (2001). Slope distributions, threshold hillslopes, and steady-state topography. *American Journal of Science*, **301**, 432–452.

Plafker, G. and Ericksen, G. E. (1978). Nevados Huascaran avalanches, Peru. In B. Voight (ed.), *Rockslides and Avalanches: I, Natural Phenomena*. Amsterdam: Elsevier, pp. 277–314.

Pratt-Sitaula, B., Burbank, D. W., Heimsath, A. and Ohja, T. (2004). Landscape disequilibrium on 1000–10,000 year scales, Marsyandi River, Nepal, Central Himalaya. *Geomorphology*, **58**, 223–241.

Schneider, J. L., Pollet, N., Chapron, E., Wessels, M. and Wassmer, P. (2004). Signature of Rhine Valley sturzstrom dam failures in Holocene sediments of Lake Constance, Germany. *Sedimentary Geology*, **169**, 1–2, 75–91.

Shang, Y., Yang, Z., Li, L. *et al*. (2003). A super-large landslide in Tibet in 2000: background, occurrence, disaster and origin. *Geomorphology*, **54**, 225–243.

Slaymaker, O. (2006). Towards the identification of scaling relations in drainage basin sediment budgets. *Geomorphology*, **80**, 8–19.

Thiery, Y., Malet, J.-P., Sterlacchini, S., Puissant, A. and Maquaire, O. (2007). Landslide susceptibility assessment by bivariate methods at large scales: application to a complex mountainous environment. *Geomorphology*, **92**, 38–59.